CrossMark

ORIGINAL PAPER

Comparison of Oxidation Behavior of Shot-Peened Plasma Spray Coatings with Cold Gas Dynamic Spray Coatings

Kadir Mert Doleker[1] · Abdullah Cahit Karaoglanli[1]

Abstract Atmospheric plasma spray (APS) process is commonly used in the production of TBCs due to low cost, and rapid and easy production. Cold gas dynamic spray (CGDS) method is an emerging coating technology which provides the desired properties such as low porosity, low oxide content, and dense structure for production of ideal metallic bond coat layer compared to APS and the other thermal spray processes. Within the context of this study, shot-peening process was applied to bond coats produced by APS technique in order to improve its microstructural properties like CGDS bond coats. TBCs having APS, CGDS, and shot-peened APS bond coats were isothermally exposed to 1100 °C for 8, 24, 50, and 100 h. Before and after oxidation tests, TBCs were examined and compared in terms of their microstructures and thermally grown oxide layer which forms at the interface of bond and top coats.

Keywords Oxidation · Shot peening · Thermal barrier coatings (TBCs) · Cold gas dynamic spray (CGDS)

Introduction

Thermal barrier coatings (TBCs) produced by plasma spraying method can be used to provide thermal insulation and oxidation protection of metallic components in advanced gas turbine jet engines such as blades and vanes [1, 2]. In many coating applications, atmospheric plasma spray (APS) technique is used due to low cost and

✉ Kadir Mert Doleker
kmdoleker@bartin.edu.tr

Abdullah Cahit Karaoglanli
cahitkaraoglanli@gmail.com

[1] Department of Metallurgical and Materials Engineering, Bartin University, Kutlubey-Yazicilar Campus, 74100 Bartin, Turkey

high feasibility. In this process, plasma atmosphere provides to reach very high temperatures, and thus, most materials can be deposited using APS method. However, structure of the coatings produced by APS includes oxides and porosities because its application is done in open air atmosphere, and it has low spraying velocity compared to other coating techniques such as high-velocity oxy-fuel (HVOF) and cold gas dynamic spray (CGDS) [3]. To obtain coating structures having low porosity and oxide content, CGDS technique is preferred for metallic coatings in recent years. CGDS process is applied under inert atmosphere and low-temperature conditions, and also, it reaches to very high particle velocity which provides plastic deformation effect [4]. In TBC system, bond coat layer is widely deposited by MCrAlY (M = Co, Ni or both of them) which provides oxidation and corrosion resistance as well as good adhesion between top coat and substrate [5, 6].

In high-temperature condition, TBCs are exposed to some failure mechanism like oxidation, hot corrosion, or thermal shock. Oxidation occurs through diffusion of oxygen from top coat to bond coat. Bond and top coat layers including oxygen reservoirs such as porosity, gap or crack trigger to accelerate of oxidation of bond coat [7–10]. Oxidation, an inevitable and severe failure mechanism for gas turbine engines, causes spallation of ceramic top coating from metallic bond coating due to formation of thermally grown oxide (TGO) layer. In fact, TGO consists of primarily Al_2O_3 phase which decelerates oxygen penetration and it contributes to decrease in oxidation of bond coat [11, 12]. However, proceeded oxidation time causes formation of mixed oxides consisting of a combination of NiO, CoO, Cr_2O_3, $Ni(Cr, Al)_2O_4$ spinels due to depletion of Al in rich phases as called β-NiAl in MCrAlY bond coats. Therefore, formation of these mixed oxides leads to volume expansion and spallation of coating can occur because of crack formation in TGO layer [13, 14].

Shot-peening process is performed to machine components to increase their fatigue life. Shot peening which is applied with bombarding of small balls to material surface brings about the compressive residual stress on subsurface areas, and thus higher hardness and dense surface properties can be obtained [15]. Some experimental studies have been reported about MCrAlY coating with shot-peening process in the literature [16–18]. The data obtained after the tests on TBC systems with shot-peened metallic bond coats under high-temperature conditions indicate that the shot-peening process can be used in thermal barrier spray coating applications as a novel surface modification technique. It should be also noted that, the coating characteristics obtained though modification of APS coating surfaces through shot-peening process, are similar to superior characteristics of the coatings such as CGDS. According to analysis results, CGDS-TBCs show better oxidation performance as expected due to its superior microstructural properties. However, shot-peened TBCs exhibit oxidation performance near to CGDS-TBCs because decreasing porosity, denser surface, and lower roughness values contribute lower thickness TGO formation compared to as-sprayed APS-TBC.

Experimental Procedures

A nickel-based Inconel 718 (%53 Ni, %19 Cr, %5,5 Nb, %3 Mo, %1 Ti, Fe balance) superalloy disk-shaped samples with a diameter of 25.4 mm and a thickness of 4 mm were used as substrate material. Prior to the coating deposition of Inconel 718 substrate material, undesirable residues like contamination or impurities were removed from the surface through grit blasting. Grit blasting with 2.5 bar and angle of 75° was applied at a distance of 10 cm from the surface using Al_2O_3 grits, and then the coated samples were cleaned by ethanol in ultrasonic bath. Co38Ni32.5Cr21Al8Y0.5 (5–37 μm, Sulzer-Metco) and ZrO_2—8 wt% Y_2O_3 (YSZ) (−45 + 20 μm, GTV) were used powders were used as the feedstocks for the deposition of the metallic bond and ceramic top coats. Superalloy substrate materials were coated with CoNiCrAlY using a GTV F6 APS and a Plasma Giken CGDS systems. Thermally sprayed metallic bond coats were coated with YSZ using a GTV F6 APS system. Thickness of the bond and the ceramic top coats were measured approximately 100 and 300 μm, respectively. The spray parameters employed for depositing the TBC systems are listed in Table 1.

After the coating deposition, the CoNiCrAlY bond coating specimens have been exposed to plastic deformation via shot-peening process with Almen intensity (10–12 A) using Micropeen-Peenmatic 2000S shot-peening tool. Cast steel shots have been widely used for the applications. Almen intensity is the plastic deformation rate of shot-peening process. It is the absolute deflection value of standard Almen strips subjected to the application of certain pre-shot-peening conditions (air pressure, shot diameter, peening duration, etc.) Saturation rate is also a certain level that the reached deflection cannot be changed over than 10% whether the plastic deformation rate is increased or not. The shot-peening parameters are listed in Table 2. Afterward, shot-peened and as-deposited CoNiCrAlY coatings were coated with YSZ using APS process. Surface roughness values of the bond and ceramic top coatings were measured using the surface roughness tester (SJ-310, Mitutoyo). Hardness test of the coatings was carried out with 25-gf load (using

Table 1 Deposition parameters of bond and top coats

APS CoNiCrAlY bond coat					
Arc current	Electric power	Argon flow rate	Hydrogen flow rate	Powder feedstock rate	Gun distance
600 A	40 kW	65 slpm	14 slpm	30 g/s	140 mm
APS YSZ top coat					
Arc current	Electric power	Argon flow rate	Hydrogen flow rate	Powder feedstock rate	Gun distance
630 A	40 kW	44 slpm	13 slpm	25 g/s	90 mm
CGDS CoNiCrAlY bond coat					
Spray pressure	Gas temperature	Working gas (slpm)	Spray distance	Gun speed	
30 bar	600 °C	Helium (1000)	15 mm	20 mm/s	

Table 2 Parameters of shot-peening process

Processes parameters	Values
Almen intensity	10–12 A
Shot type	S110
Saturation rate	%100
Air pressure kPa	520

Qness, Q10 microhardness testing machine) with 15-s durations. Hardness measurements were taken from five different distances ranging between 5 and 35 μm, and then their mean value was taken as the average hardness. Microstructures of the coatings were evaluated using a scanning electron microscope (MAIA3 XMU, TESCAN). Clemex Vision Lite software program was used to observe and calculate porosity contents of the coatings. Porosity measurements of TBC systems were performed on 10 images belonging to each of the coating layer, and the microstructure of matrix and porosity structures were defined using an image analysis program. Surface roughness, porosity content, and hardness values of the coatings are shown in Table 3.

Results and Discussion

Cross-sectional microstructure of the TBC samples were studied by SEM equipped with energy-dispersive X-ray spectrometer (EDS). The samples were cut into small pieces by the slow-speed saw and then cleaned by the ethanol. Then the samples were mounted for metallographic preparation. The grinding and polishing of the samples were performed. Diamond paste was used for rough and fine polishing. The bond coat structure of as-sprayed CoNiCrAlY, and the bond coat structure shot-peened specimen are shown in Fig. 1. As seen from the microstructures, the as-sprayed APS bond coat has a high porosity and oxide content beside its rough surface structure. On the other hand, the shot-peened bond coat has a lower surface roughness and oxide content and exhibits a dense coating structure within a wide region starting from the surface and extending to lower areas. Figure 2 shows typical cross-sectional morphologies of the as-sprayed TBC systems comprising CoNiCrAlY bond and YSZ top coats. As seen in Fig. 2 a, the coatings deposited

Table 3 Surface roughness, porosity content, and hardness values of coatings

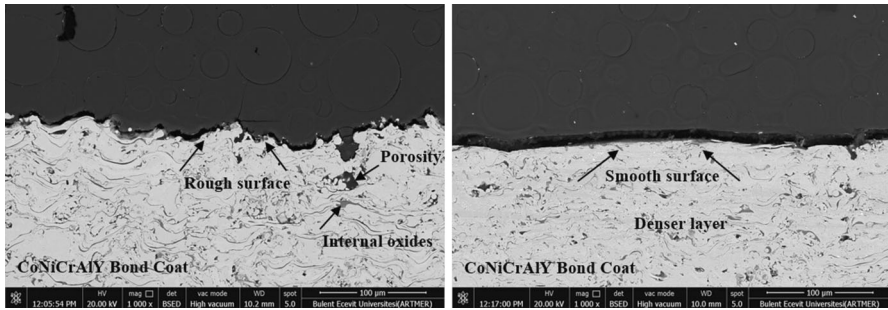| Coatings	Surface roughness (μm)	Porosity (%)	Hardness (Hv)
APS bond coat	7.3 ± 0.6	8.0 ± 2.0	350 ± 25
Shot-peened APS bond coat	2.8 ± 0.3	6.4 ± 2.0	515 ± 30
CGDS bond coat	9.2 ± 0.5	1.3 ± 1.0	550 ± 60
APS top coats	5.2 ± 0.1	7.2 ± 0.9	700 ± 50

Fig. 1 SEM cross-sectional microstructures of CoNiCrAlY bond coats. **a** APS; **b** shot-peened APS
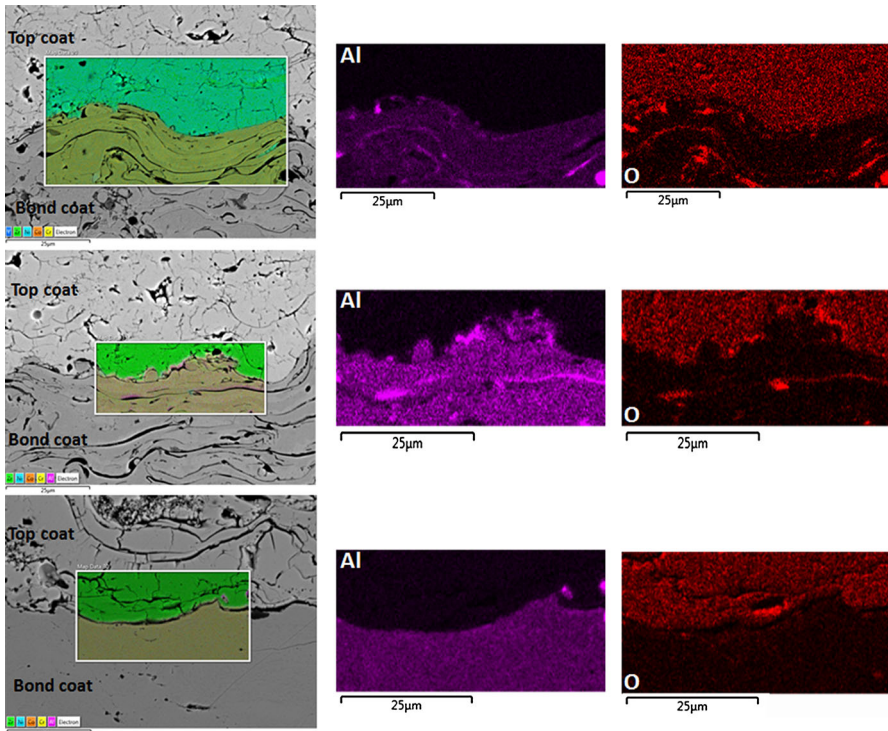

Fig. 2 SEM cross-sectional microstructures of TBCs. **a** APS; **b** shot-peened APS and **c** CGDS bond coats

with APS technique involve several crack, porosity, and oxide formations as commonly encountered in conventional plasma spray coatings. On the other hand, the shot-peened APS bond coat shown in Fig. 2b exhibits a denser structure with less porosity at the regions close to the top coat interface, as a result of emerging plastic deformation effect. A lower rate of roughness with a smoother surface was obtained as a result of plastic deformation applied on the surface. The CGDS bond

coats shown in Fig. 2c have a dense structure without oxides and with low porosity. In the elemental mapping analyses given in Fig. 2, CGDS bond coat structure has uniform Al content, whereas APS coatings exhibit a non-uniform distribution of Al. This directly affects the characteristic properties of the oxides forming at the coating interface under oxidation conditions, thus having a major effect on the service life of the coating and occurrence of failures [19]. The shot-peened APS coatings exhibit a more uniform Al content compared to conventional APS coating structure, which in turn yields superior coating characteristics similar to CGDS coating.

In Fig. 3, the effect of shot-peening process on the hardness of the coatings is shown in terms of influenced depth. Hardness of CGDS coatings varies uniformly as from the coating surface, exhibiting the highest hardness values as a result of production-related and microstructural features of the process. Hardness of APS coating is as expected from conventional plasma spray coating structure. As seen in the graph, the influence of shot peening applied on APS coatings maintains its effect up to a remarkable depth of 35 μm, resulting in a significant rise in the hardness values of the coatings within this distance.

The bond–top coat interface microstructures of TBC system with APS bond coat are obtained after the oxidation tests at 1100 °C for different test periods, and its elemental mapping analysis performed after 100 h period is given in Figs. 4 and 5. Formation of TGO layer is visible at the interface as a result of diffusion of oxygen as from the initial stages of oxidation. The thickness of TGO layer increased with increasing time period. The TGO formation lost its integrity after the first 8-h oxidation period, leading to emergence of a dominant Al_2O_3 oxide content along with Cr_2O_3 and other oxide formations. As the β phase is depleted in the areas close to the interface, diffusion of Al from lower regions becomes harder. After this point, instead of Al, other metals such as Ni and Co within the γ matrix start to oxidize and form the spinels [7, 20, 21]. As the Al and Cr elements become depleted due to isothermal oxidation, Ni starts to react with oxygen and Al_2O_3 to form spinels in the TGO layer between the top and the bond coats after 24-h isothermal oxidation
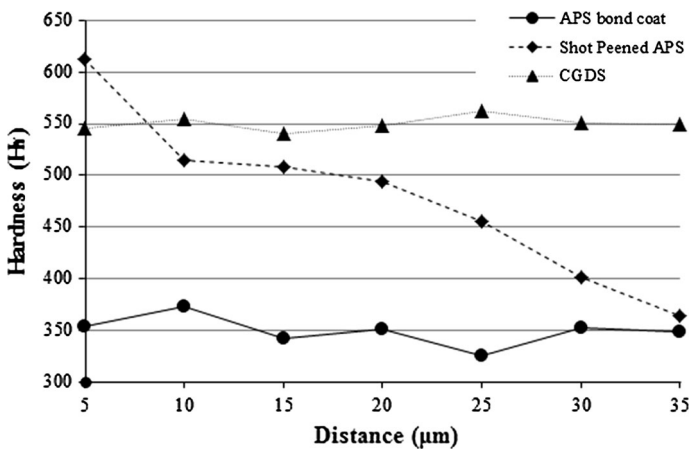

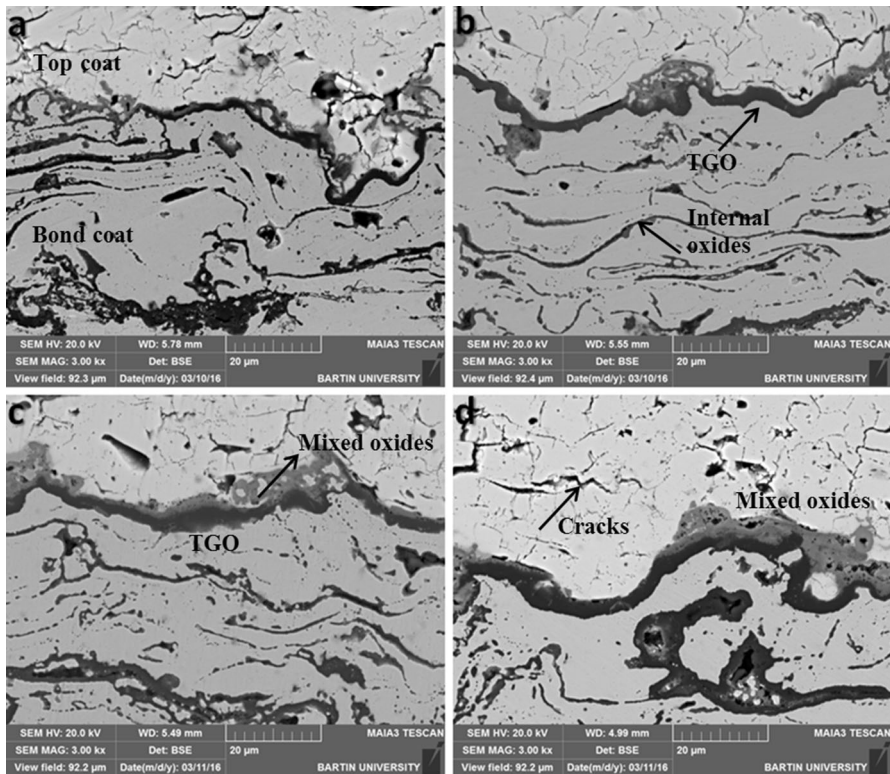Fig. 3 Effect of the shot-peening process on the hardness depending on the distance from the surface

Fig. 4 Cross-sectional SEM images of APS-TBCs after isothermal oxidation at 1100 °C. **a** 8 h; **b** 24 h; **c** 50 h and **d** 100 h
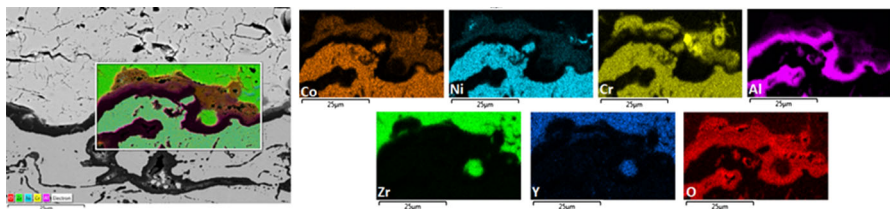

Fig. 5 Cross-sectional SEM elemental maps images of APS-TBCs after isothermal oxidation at 1100 °C for 100 h

(Fig. 4b). Formation of oxides and spinels other than Al_2O_3 were also observed in the TGO structure with increasing time in previous studies [22, 23].

The bond–top coat interface microstructures of TBC system with shot-peened APS bond coat obtained after the oxidation tests at 1100 °C for different test periods, as well as its elemental mapping analysis performed after 100-h period are given in Figs. 6 and 7. The interface images of shot-peened APS-TBC system after oxidation test reveal a smoother interface as compared to conventional APS-TBC system. Formation of TGO structure started at initial stages of oxidation; however, it
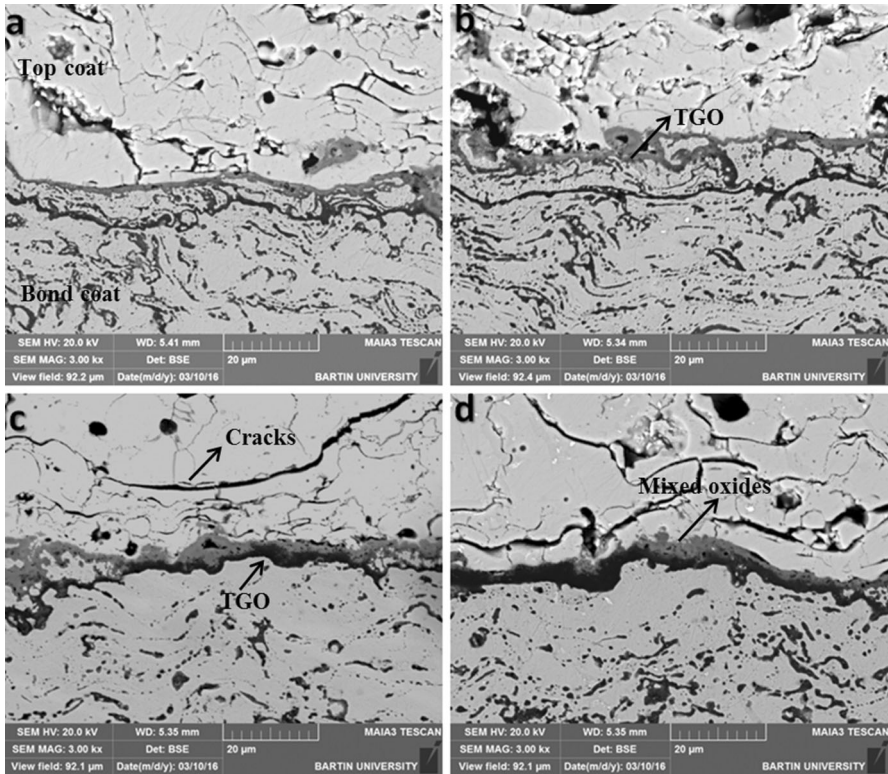
Fig. 6 Cross-sectional SEM images of shot-peened APS-TBCs after isothermal oxidation at 1100 °C. **a** 8 h; **b** 24 h; **c** 50 h and **d** 100 h
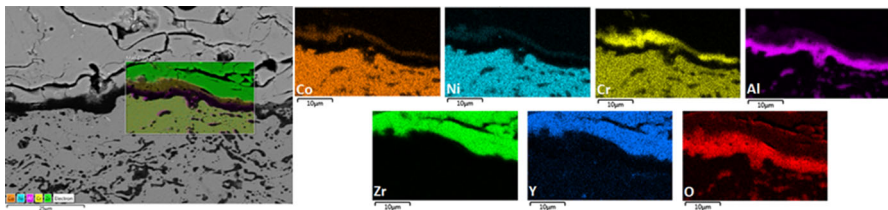

Fig. 7 Cross-sectional SEM elemental maps images of shot-peened APS-TBCs after isothermal oxidation at 1100 °C for 100 h

did not exhibit a growth proportional with increasing time as encountered in conventional APS-TBC system. Researchers believe porous structure of coatings lead to the emergence of a free path for oxygen penetration and corrosive ions inside the coating that increases the oxidation rate [24, 25]. As a result of the dense structure obtained in the surface and its vicinity after the shot-peening process, the rate of oxygen penetration through the surface is reduced, and the oxidation process is slowed down. This is attributed to the fact that the dense coating structure obtained through plastic deformation effect as a result of shot-peening process

slowed down the penetration of oxygen diffusing from the surface, thus enabling formation of a more uniformly distributed Al at the interface.

The bond–top coat interface microstructures of TBC system with CGDS bond coat obtained after the oxidation tests at 1100 °C for different test periods, as well as its elemental mapping analysis performed after 100-h period are given in Figs. 8 and 9. The TGO structure forming at the interface of the TBC system with CGDS-deposited bond coats, exhibit a more uniform structure here. The dominant content within the resulting TGO structure is Al_2O_3. Traces of mixed oxide formations are visible in some regions after 100-h oxidation period.

The CoNiCrAlY structure that forms the TBC system produced with CGDS technique consists of Ni-Co based γ-matrix and β-precipitates with (Co,Ni)Al content. The Al-rich β-precipitate exhibits an oxidation-dependent formation and disappears as a result of time-dependent reduction in Al concentration. This precipitate formation is not observed in other TBC systems produced with APS technique, due to the high oxide content related with deposition conditions, as well as low Al concentration of the bond coat. This is attributed to open-atmosphere deposition conditions. Due to their dense and uniform structure, the coatings deposited with CGDS technique are favored in high-temperature applications. They
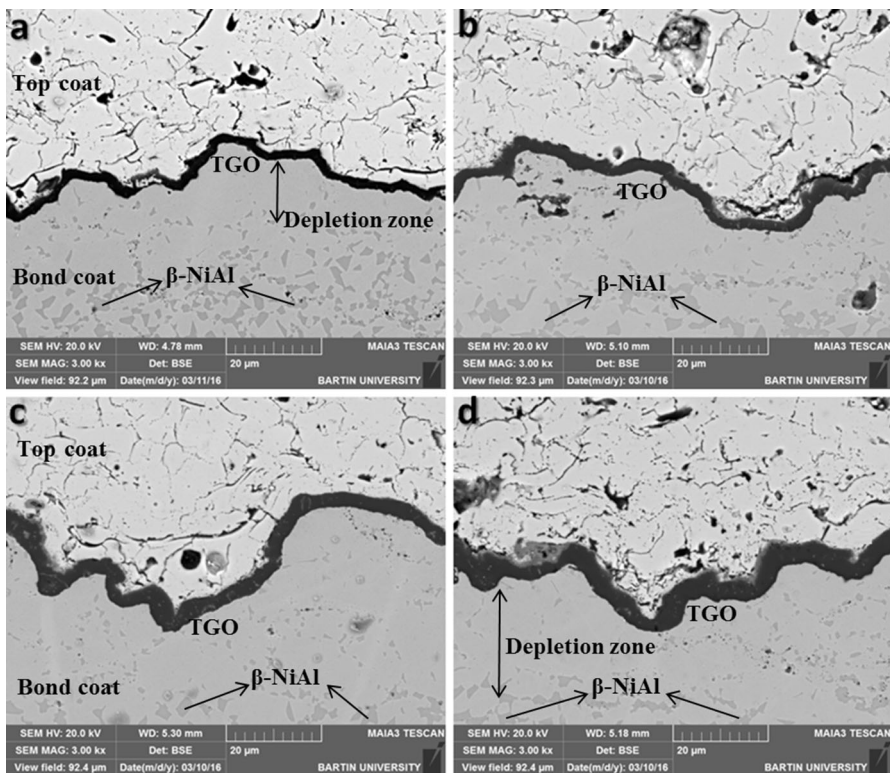

Fig. 8 Cross-sectional SEM images of CGDS-TBCs after isothermal oxidation at 1100 °C. **a** 8 h; **b** 24 h; **c** 50 h and **d** 100 h
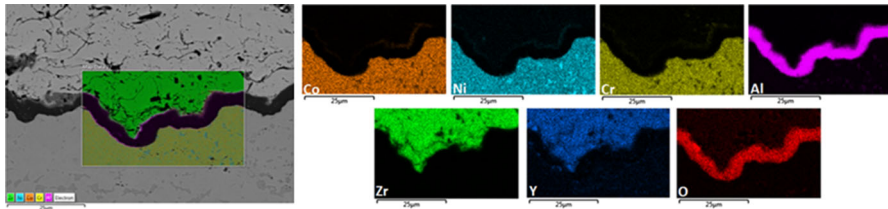
Fig. 9 Cross-sectional SEM elemental maps images of CGDS-TBCs after isothermal oxidation at 1100 °C for 100 h

feature significantly lower rates of oxide and porosity content as compared to APS coatings since CGDS deposition conditions are based on plastic deformation rather than melting of powder particles, thus allowing low-temperature process conditions.

During the oxidation of TBC systems, the Al in the bond coat with MCrAlY content, binds with oxygen and leads to formation of α-alumina and TGO. The Al here comes from β-precipitates. The Al in β phase diffuses toward TGO and oxides. However, after a period, the Al-rich phase starts to lose its Al content which in turn enables formation of different oxides within the TGO structure [7, 22, 26, 27].

Formation of Al-poor regions was observed in some of the researches after a specific oxidation period. Diffusion of Al from lower regions is obstructed as the β phase disappears near the surface. After this point, metals such as Ni and Co, instead of Al, start oxidizing on the surface and form spinels [7, 22]. Spinels are generally located locally and cause rapid volumetric changes in addition to their porous-fragile structure, all of which endanger the integrity of TGO [28]. Besides, with the assistance of inter-connected cracks in the as-sprayed ceramic top coat, oxygen migrates swiftly from surface of the top coat to the bond coat [21]. These microstructural features are a consequence of the deposition processes [29].

At initial stages of oxidation, after the oxidation of Al, Al is diffused to Al-poor surface from Al-rich regions under bond coat, as the amount of Al decreased in the surface. Here, Al-rich region refers to the regions with β-NiAl precipitates. However, after longer periods of oxidation, transformation of β precipitates NiAl into γ-NiAl$_3$ with Al depletion and the distance for diffusion of Al increased, and accordingly, Al depletion regions emerged [30]. In the literature, it was reported that the Al-rich β phase is gradually consumed due to two effects: surface oxidation and coating–substrate interdiffusion. In addition, the researchers specified that some voids and oxides along the coating–substrate interface, or inside the coating, were considered to play a role in blocking the diffusion of alloying elements [31]. In the present study, Al depletion regions were not observed in the TBC systems produced with APS technique whereas they started to emerge in TBC systems deposited with CGDS technique after an oxidation period of 50 h at a depth of approximately 20 μm.

Conclusions

In the present work, the microstructure and oxidation behavior of the three different TBC systems including a CoNiCrAlY bond coat and an 8YSZ top coat have been studied, and the following conclusions are drawn:

Different TBC systems were successfully produced using APS and CGDS techniques. Shot peening process was successfully used in enhancement of bond coat surface characteristics of TBC systems. Application of shot-peening process was found to be decreasing the surface roughness of APS coating with high oxide, porosity and crack content, thus enabling achievement of a denser coating structure. Shot-peening process was found to maintain its effect up to a depth of 35 μm, leading to a significant rise in hardness values of the coating along this depth. In the analysis of oxidation mechanism of TBC systems produced with APS, CGDS, and shot-peening processes, the TGO of TBC system produced with CGDS technique exhibits a uniform structure with Al_2O_3 content, which is favored. On the other hand, the TGO structure of TBC system produced with APS technique has high oxide content with a non-uniform distribution. In the analysis of oxidation behavior of coatings with shot-peened surfaces, penetration of oxygen diffused from the surface into lower layers was found to decrease, as a result of dense coating structure and decline in the surface roughness which in turn leads to a smoother surface structure. Consequently, a more uniform TGO layer with lower oxide formation and a dense structure was obtained. In the present study, the coating performance of TBC systems produced with conventional APS technique under isothermal oxidation conditions was compared with that of the specimens produced with CGDS process, which is recently adopted as an alternative coating process with its superior properties. The TBC system produced with CGDS technique evidently over-performed the TBC system produced with APS technique under high-temperature service conditions. As the price of its superior performance, CGDS process is a much costlier technique in terms of the used equipment, gas and other issues, as compared to APS technique. On the other hand, the APS bond coat structure, surface characteristics of which is modified with shot-peening process in the present study, exhibited a superior performance under high-temperature conditions as similar to the TBC system produced with CGDS technique. Thus, modification of the surface characteristics of plasma spray process, as a simple and cost-efficient thermal spray coating method, with the shot-peening process, can be used as an alternative technique in thermal spray coating applications.

References

1. R. A. Miller, *Journal of Thermal Spray Technology* **6**, (35–42) 1997.
2. P. Audigié, S. Selezneff, A. R. V. Put, C. Estournès, S. Hamadi and D. Monceau, *Oxidation of Metals* **81**, (33–45) 2014.

3. S. Bose, *High Temperature Coatings* (Elsevier, Burlington, 2007), pp. 253–273.
4. P. Richer, M. Yandouzi, L. Beauvais and B. Jodoin, *Surface and Coatings Technology* **204**, (3962–3974) 2010.
5. A. Vande Put, D. Oquab, E. Péré, A. Raffaitin and D. Monceau, *Oxidation of Metals* **75**, (247–279) 2011.
6. A. C. Karaoglanli, E. Altuncu, I. Ozdemir, A. Turk and F. Ustel, *Surface and Coatings Technology* **205**, (369–373) 2011.
7. A. G. Evans, D. R. Mumm, J. W. Hutchinson, G. H. Meier and F. S. Pettit, *Progress in Materials Science* **46**, (505–553) 2001.
8. V. K. Tolpygo and D. R. Clarke, *Surface and Coatings Technology* **200**, (1276–1281) 2005.
9. Z. Derelioglu, A. L. Carabat, G. M. Song, S. van der Zwaag and W. G. Sloof, *Journal of the European Ceramic Society* **35**, (4507–4511) 2015.
10. F. Nozahic, D. Monceau and C. Estournès, *Materials and Design* **94**, (444–448) 2016.
11. K. Ma and J. M. Schoenung, *Surface and Coatings Technology* **205**, (5178–5185) 2011.
12. W. R. Chen, X. Wu, B. R. Marple, R. S. Lima and P. C. Patnaik, *Surface and Coatings Technology* **202**, (3787–3796) 2008.
13. G. Pulci, J. Tirillò, F. Marra, F. Sarasini, A. Bellucci, T. Valente and C. Bartuli, *Surface and Coatings Technology* **268**, (198–204) 2015.
14. C. Zhu, P. Li and X. Y. Wu, *Ceramics International* **42**, (7708–7716) 2016.
15. K. Dai, J. Villegas, Z. Stone and L. Shaw, *Acta Materialia* **52**, (5771–5782) 2004.
16. N. L. Liyong, W. U. Zilong and Z. Chungzen, *Progress in Natural Science: Materials International* **21**, (173–179) 2011.
17. A. Gil, V. Shemet, R. Vassen, M. Subanovic, J. Toscano, D. Naumenko, L. Singheiser and W. J. Quadakkers, *Surface and Coatings Technology* **201**, (3824–3838) 2006.
18. L. Yong, C. J. Li, L. K. Xing and G. J. Yang, *Journal of Thermal Spray Technology* **20**, (121–131) 2011.
19. A. Manap, A. Nakano and K. Ogawa, *Journal of Thermal Spray Technology* **21**, (586–596) 2012.
20. D. Renusch, M. Schorr and M. Schütze, *Materials Corrosion* **59**, (547–555) 2008.
21. Y. Z. Liu, S. J. Zheng, Y. L. Zhu, H. Wei and X. L. Ma, *Journal of the European Ceramic Society* **36**, (1765–1774) 2016.
22. H. J. Jang, D. H. Park, Y. G. Jung, J. C. Jang, S. C. Choi and U. Paik, *Surface and Coatings Technology* **200**, (4355–4362) 2006.
23. M. Saremi, A. Afrasiabi and A. Kobayashi, *Transactions of JWRI* **36**, (41–45) 2007.
24. F. Naeimi, M. R. Rahimipour and M. Salehi, *Oxidation of Metals* **86**, (59–73) 2016.
25. K. Tao, X. L. Zhou, H. Cui and J. S. Zhang, *Transactions of Nonferrous Metals Society of China* **19**, (1151–1160) 2009.
26. M. Hasegawa and Y. Kagawa, *International Journal of Applied Ceramic Technology* **3**, (4), (293–301) 2006.
27. T. Koomparkping, S. Damrongrat and P. Niranatlumpong, *Journal of Thermal Spray Technology* **14**, (264–267) 2004.
28. Y. Li, C. J. Li, Q. Zhang, G. J. Yang and C. X. Li, *Journal of Thermal Spray Technology* **19**, (1–2), (168–177) 2010.
29. A. C. Fox and T. W. Clyne, *Surface and Coatings Technology* **184**, (311–321) 2004.
30. L. Ajdelsztajn, F. Tang, G. E. Kim, V. Provenzano and J. M. Schoenung, *Journal of Thermal Spray Technology* **14**, (23–30) 2003.
31. K. Yuan, R. Eriksson, R. Peng, X. H. Li, S. Johansson and Y. Wang, *Surface and Coatings Technology* **232**, (204–215) 2013.